THE
UNIVERSITY
OF RHODE ISLAND

University of Rhode Island

DigitalCommons@URI

2-11-2021

Net volatilization of PAHs from the North Pacific to the Arctic Ocean observed by passive sampling

Haowen Zheng

Minggang Cai

Wenlu Zhao

Mohammed Khairy

Mian Chen

See next page for additional authors

Follow this and additional works at: https://digitalcommons.uri.edu/gsofacpubs

This is a pre-publication author manuscript of the final, published article.

Authors

Haowen Zheng, Minggang Cai, Wenlu Zhao, Mohammed Khairy, Mian Chen, Hengxiang Deng, and Rainer Lohmann

Net volatilization of PAHs from the North Pacific to the Arctic Ocean observed by Passive sampling

Haowen Zheng [a, b]; Minggang Cai [a, b]; Wenlu Zhao [c]; Mohammed Khairy [d, e]; Mian Chen [a, b]; Hengxiang Deng [a, b]; Rainer Lohmann [d, *]

[a] *State Key Laboratory of Marine Environmental Science, Xiamen University, Xiamen 361102, China*

[b] *College of Ocean and Earth Science, Xiamen University, Xiamen 361102, China*

[c] *School of Environmental Science and Engineering, Zhejiang Gongshang University, Hangzhou 310018, China*

[d] *Graduate School of Oceanography, University of Rhode Island, Narragansett, Rhode Island 02882-1197, United States*

[e] *Department of Environmental Sciences, Faculty of Science, Alexandria University, 21511 Moharam Bek, Alexandria, Egypt*

*Corresponding author: Rainer Lohmann

E-mail: rlohmann@uri.edu

Abstract

The North Pacific-Arctic Oceans are important compartments for semi-volatile organic compounds' (SVOCs) global marine inventory, but whether they act as a "source-sink" remains controversial. To study the air-sea exchange and fate of SVOCs during their poleward long-range transport, low-altitude atmosphere and surface seawater were measured for polycyclic aromatic hydrocarbons (PAHs) by passive sampling from July to September in 2014. Gaseous PAH concentrations (0.67-13 ng m^{-3}) were dominated by phenanthrene (Phe) and fluorene (Flu), which displayed an inverse correlation with latitude, as well as a significant linear relationship with partial pressure and inverse temperature. Concentrations of PAHs in seawater (1.8-16 ng L^{-1}) showed regional characteristics, with higher levels near the East Asia and lower values in the Bering Strait. The potential impact from the East Asian monsoon was suggested for gaseous PAHs, which – similar to PAHs in surface seawater - were derived from combustion sources. In addition, the data implied net volatilization of PAHs from seawater into the air along the entire cruise; fluxes displayed a similar pattern to regional and monthly distribution of PAHs in seawater. Our results further emphasized that air-sea exchange is an important process for PAHs in the open marine environments.

1. Introduction

Polycyclic aromatic hydrocarbons (PAHs) are ubiquitous in the environments worldwide, and some of them are toxic, carcinogenic and mutagenic (Bozlaker et al., 2008; Okona-Mensah et al., 2005; Perera et al., 2005). Besides their petrogenic origin, PAHs are also generated during the incomplete combustion of organic materials, like fossil fuels and biomass (Yunker et al., 2002). As a class of semi-volatile organic compounds (SVOCs), they could arrive in the polar area from temperate regions with subsequent deposition and re-volatilization, representing an emerging concern in the Arctic like other conventional pollutants (Cai et al., 2016; Friedman and Selin, 2012; Laender et al., 2011).

Atmospheric transport has been considered the primary pathway for PAHs transported from the lower latitudes to the Arctic environments (Mulder et al., 2015; Dotel et al., 2020). Previous studies showed that PAHs found in the Arctic seawater and sediments mainly originated from natural underwater hydrocarbon seeps, while those in the air were from atmospherically derived sources (Harvey et al., 2014; Yunker et al., 2011; Foster et al., 2015). With the concern of climate change, the "polar sinks" for many conventional pollutants may become secondary sources via air-water exchange, that is, the declining sea ice coverage and rising temperature could lead to an accelerating release of PAHs from sea ice and seawater to the atmosphere (Hung et al., 2010; Ma et al., 2011, 2013; Galban-Malagon et al., 2013). Thus, studying PAHs in the atmosphere and related interfaces is helpful to better know the current state of the PAH emission and their fates in the Arctic (Friedman et al., 2014).

Passive sampling is an effective monitoring technique for SVOCs, which is easy to operate, cost-effective and with high enrichment of the target compounds, and has been applied in various global monitoring projects (Lohmann et al., 2001; Harner et al., 2003; Meijer et al., 2003; Jaward et al., 2004; Khairy and Lohmann, 2014; Mcdonough et al., 2014; Zhao et al., 2018). This method integrates contaminant concentrations over time, representing time-weighted averages (Stuer-Lauridsen, 2005; Shaw and Mueller, 2009; Wania and Shunthirasingham, 2020). For PAHs, the freely-dissolved pollutants can be sampled with low-density polyethylenes (LDPEs) (Khairy and Lohmann, 2014). Concentrations of target compounds that do not reach equilibrium during the exposure period can be estimated relying

64   on the diffusive loss of performance reference compounds (PRCs) (Booij et al., 2002; Mayer et

65   al., 2003; Khairy and Lohmann, 2012).

66   Although previous studies have reported the distribution and direction of PAHs air-water

67   exchange in the northern Pacific and the Arctic, as well as fugacity model simulations, the

68   seasonal and regional trends of PAHs remain uncertain (Ke et al., 2017; Ma et al., 2013). Hence

69   the air-sea exchange process of PAHs from the North Pacific to the Arctic needs further research.

70   In this study, we performed spatially resolved air and water measurements during the sampling

71   cruise, and the objectives were to (1) obtain the spatial and temporal distribution characteristics

72   of atmospheric and dissolved PAHs in seawater from the North Pacific Ocean to the western

73   Arctic Ocean; (2) assess the source of gaseous and freely dissolved PAHs at most sites; (3)

74   derive the direction and magnitude of the air-sea flux exchange process of PAHs.

75   **2. Materials and methods**

76   **2.1 Area description**

77   During the Chinese sixth Arctic scientific expedition cruise from July to September in

78   2014, we collected 32 atmosphere and 16 surface seawater samples in the Japan Sea, Bering

79   Sea and Chukchi Sea onboard the R/V *Xuelong* (Snow Dragon). The Bering Strait, connecting

80   the Bering Sea with the Chukchi Sea, and linking the Asian and American continents, is the

81   boundary of the Arctic and Pacific Oceans. The Bering Sea is a semi-enclosed, high-latitude

82   sea that is almost divided equally between a deep basin (maximum depth 3500 m) and the

83   continental shelves (<200 m). The eastern broad (>500 km) shelf of the Bering Sea contrasts

84   with the narrow (<100 km) western shelf (Stabeno and Van Meurs, 1999). Water in the vast

85   (~500 km wide from east to west and ~800 km long from north to south) and shallow (~50 m)

86   Chukchi Sea (Arctic Ocean) is strongly forced by Pacific Ocean water entering through the

87   Bering Strait (Woodgate et al., 2005), which delivers heat, freshwater, nutrients, and carbon to

88   the Chukchi shelf and the Arctic Ocean.

89   In this study, there were 16 sampling stations (Table S1 in Supporting Information, SI), of

90   which PS-01 to PS-07 were located in the Sea of Japan and northwest Pacific Ocean, while PS-

91   08 to PS-10 in the Bering Sea and the Bering Straits, and PS-11 to PS-16 in the Arctic Ocean

92   (mainly in Chukchi Sea).

2.2 Materials Preparation and Field sampling

2.2.1 Preparation for LDPEs

Both atmospheric and seawater samplers were made of LDPEs with PRCs, which is similar to the material used in semipermeable membrane devices; The inclusion of PRCs provided a means to identify the absorption of hydrophobic PAHs by estimating dissipation rates of PRCs (Booij et al., 2002; Lei et al., 2020). LDPEs (10 cm × 40 cm size, 50 μm thickness) were cleaned in dichloromethane and n-hexane for 24 h respectively. Deuterated PAHs (pyrene-d_{10} and benzo [a] pyrene-d_{12}, namely Pyr-d_{10} and BaP-d_{12}) were used as PRCs to infer the equilibrium concentration of compounds in the passive samplers as in previous work (Booij et al., 2002; Mcdonough et al., 2014). LDPEs were soaked in PRCs and continuously shaken for one month to achieve homogenous uptake prior to deployments.

2.2.2 Simultaneous sampling in atmosphere and surface seawater

Atmospheric and surface-seawater LDPEs were deployed and collected simultaneously on the underway R/V *Xuelong* in the Japan, Bering and Chukchi Seas (Fig. S1), and LDPEs were changed every three days. The sampling site coordinates were calculated as the middle position of the start and end of sampling positions.

Surface-seawater LDPEs were put into a stainless-steel pipe, and continuously exposed to fresh marine surface seawater from the onboard seawater supply. We controlled the flow rate of the seawater such that the LDPEs were submerged constantly. The atmospheric sampling device was installed on the top deck, which was about 26 m above sea level. The device consisted of two stainless-steel bowls, connected in the middle by a stainless-steel center shaft. The LDPEs, thread on a metal wire, were fastened on the center shaft for sampling. All the LDPE samples were sealed with an aluminum foil bag and stored at -20ºC.

2.2.3 Other auxiliary parameters

Auxiliary parameters such as temperature and salinity were provided by the *Xuelong* ship real-time monitoring system, and other parameters such as wind speed, wind direction and air temperature were provided by the automatic weather station on board *Xuelong* ship.

2.3 Pretreatment and analysis

LDPE samples were thawed out at room temperature, then cleaned with Milli-Q water and

122   any excess water or biofouling was removed with KimWipes. 200 mL of n-hexane was added

123   to completely cover LDPEs after addition of 50 μL 100 ppb PAHs recovery indicator surrogates

124   (acenaphthalene-d_{10}, phenanthrene-d_{10}, chrysene-d_{12} and perylene-d_{12}, namely Acp-d_{10}, Phe-d_{10},

125   Chry-d_{12} and Pery-d_{12} respectively). After extraction for 24 h, the n-hexane was decanted and

126   the extract was kept in a clean glass bottle. After a solvent exchange to dichloromethane, and

127   repeating the above steps, extracts were combined. The extract was concentrated to 1mL in a

128   30°C water bath by a fully automatic sample concentrator, transferred to a volumetric tube and

129   slowly purged to 100 μL with high-purity nitrogen. Then 50 ng of deuterated terphenyl and 35

130   ng of 2, 4, 6-Tribromobiphenyl were added as internal standards. The extract was sealed and

131   frozen for storage before analysis. The weight of the extracted LDPE samples was recorded

132   before and after treatment.

133   An Agilent 6890-5973 GC-MS equipped with a DB5-MS quartz capillary column (30 m

134   × 0.25 mm i.d. × 0.25 μm, J&W Scientific Inc., Folsom, U.S.A.) was used to detect PAHs. The

135   high purity helium was used as carrier gas with the flow rate of 1mL min^{-1}. The temperature

136   programming of chromatography column started at 90 °C with three 3 minutes hold, then

137   reached 110 °C at 5 °C min^{-1}(holding 2 minutes), increased by 8 °C min^{-1} until 200 °C (holding

138   3 minutes), and finally reached 315 °C at 5 °C min^{-1}fiv, keeping the final temperature for 5

139   minutes.

140   **2.4 Quality assurance and quality control**

141   Avoiding contamination was an important consideration in all steps associated with the

142   extraction and analysis of LDPEs. All glassware used during pretreatment were cleaned, baked

143   at 450°C for at least 4 hours, and thoroughly solvent-rinsed before use. The field blanks were

144   regularly included in the sampling protocol, and included when samplers were changed during

145   deployment and retrieval. Method detection limits (MDLs) were calculated as three times the

146   standard deviation of the average field blank concentration. The MDL of the target compounds

147   are listed in SI as well as instrument detection limits. All of the data were blank-corrected.

148   When the concentration of the target compounds was less than the detection of limits, half of

149   MDL was taken as its concentration value (Antweiler and Taylor, 2008).

150   22 PAHs were detected in this study. In addition to the 16 priority PAHs listed by U.S.

151　EPA, the other six compounds were Biphenyl (Biph), 1-Methylphenanthene (1-MePhe), Retene

152　(Ret), Benzo[e]pyrene (BeP), Perylene (Pery) and Benzo[j]fluoranthene (BjF) (Table S2 in SI).

153　Due to the high environmental background concentration of naphthalene, it will not be

154　discussed in this study. In order to improve the quality and credibility of the data, if the

155　concentration of a certain target compound was greater than MDL but detected at less than 20%

156　of the total sites, it was omitted from the discussion. A total of nine PAHs in atmospheric

157　samples were regularly detected, which included phenanthrene (Phe), fluorene (Flu), Phe,

158　anthracene (Ant), 1-MePhe, fluoranthene (FluA), pyrene (Pyr), chrysene (Chry),

159　benzo[b]fluoranthene (BbF)/ benzo[k]fluoranthene (BkF) (because the peaks of BbF and BkF

160　were hard to chromatographically separate, the total concentration of BbF/BkF are reported).

161　While 11 PAHs in surface seawater samples were effectively detected, which included Flu, Phe,

162　Ant, 1-MePhe, FluA, Pyr, Chry, Biph, benz[a]anthracene (BaA), BbF/BkF. Concentrations of

163　PAHs in the samples were blank-corrected for the amounts detected in the field blanks, but not

164　recovery corrected. The average recovery rates of the four surrogates that Acp-d_{10}, Phe-d_{10},

165　Chry-d_{12}, and Pery-d_{12} were 70 ± 12, 75 ± 15, 85 ± 13, and $74 \pm 18\%$ respectively.

166　　　For the uncertainty analysis, it is difficult to estimate the overall uncertainty of air-water

167　exchange by passive sampling, because it involves multiple mathematical functions and values

168　that have both normal and lognormal errors associated with them. Additionally, the

169　uncertainties in H^{θ} are not well characterized, causing the uncertainty associated with the

170　temperature- and salinity corrections were not included.

171　**2.5 Calculations and data analysis**

172　**2.5.1 Calculations of PAH concentrations**

173　　　For each compound, the fraction of equilibrium (f) achieved for each compound was

174　determined by fitting the equilibrium of the PRCs using temperature-corrected air-water

175　partitioning coefficient in LDPEs (K_{PE}) values to a model curve derived from equation (1) (Liu

176　et al., 2016),

177　$$f = 1 - e^{-\frac{R_s t}{K_{PE} M_{PE}}} \tag{1}$$

178　　　Where R_s (L day^{-1}) is the sampling rate defined as the volume of water or air that comes

179　into contact with the sampler per day; t is deployment time (days); M_{PE} is the PE weight (kg);

180   the values of R_s can be estimated using nonlinear least squares methods, by considering f as a

181   continuous function of K_{PE}, with R_s as an adjustable parameter using Excel Solver to obtain the

182   best fit (Booij and Smedes, 2010). The average gaseous sampling rate of PAHs was 1 700 ± 1

183   500 m^3 day^{-1}, among which the Pacific Ocean and the Bering Sea was 620 ± 410 m^3 day^{-1},

184   however the Arctic Ocean was 3 100 ± 1 300 m^3 day^{-1}, resulted from different wind speed and

185   directions described below. The aqueous sampling rate of PAHs was 140 ± 54 L day^{-1}.

186   Gaseous and freely dissolved concentrations, $C_{A/W}$ of compounds were calculated from

187   the equation (2),

188   $$C_{A/W} = \frac{c_{PE} - c_{Blank}}{K_{PE}\left(1 - e^{-\frac{R_s t}{K_{PE} M_{PE}}}\right)} \tag{2}$$

189   Where C_{PE} is the PE-normalized concentrations. For more details, see the Supporting

190   Information.

191   **2.5.2 Brief description of calculation and two-film model**

192   The Whitman two-film resistance model was used for the air-sea exchange flux (F_{aw})

193   calculation in the modified version (Liss and Slater, 1974).

194   $$F_{a/w} = v_{a/w}\left(C_w - \frac{C_a}{K_{aw}}\right) \tag{3}$$

195   where $F_{a/w}$ is calculated with the mass transfer velocity ($v_{a/w}$), the concentrations in seawater

196   and atmosphere, C_w and C_a, and air-water partitioning coefficient corrected by ambient

197   temperature, K_{aw} (Liu et al., 2016). Calculation details of PAHs air-sea exchange fluxes at

198   different sites are listed in SI from Table S6 to S12.

199   **2.6 Air mass back trajectories**

200   The NOAA's HYSPLIT model was used to track the origins of air masses (Draxler and

201   Hess, 1998). Air mass back trajectories were set as 12 h steps that traced back the air masses

202   for 5 days, using the sampling height as arrival height.

203

3. Results and discussion

3.1 PAHs in the atmosphere

3.1.1 Concentrations and distributions

Total gaseous concentrations of $\sum_9$PAH ranged from 0.67 to 13 ng m^{-3} with the mean value of 3.7 ± 3.0 ng m^{-3}, close to previous data of 0.93-93 ng m^{-3} for Σ_{15}PAH reported over the North Pacific and Arctic Ocean in 2003, as well as 0.91-7.4 ng m^{-3} with a mean of 3.3 ± 1.7 ng m^{-3} for Σ_{18}PAH reported in 2010 (Ding et al., 2007, Ma et al., 2013). Observation showed the maximum concentrations occurred at PS-01 located in the Bohai Sea, and lowest at PS-16 in the Arctic Ocean (Fig. 1, Table S3).

In this study, nine different PAHs were regularly detected in most gaseous samples, including three-ring PAHs like Flu, Phe, 1-MePhe, Ant, and four-ring PAHs like FluA, Pyr, and Chry. Higher molecular weight PAH concentrations in the atmosphere were typically below their limits of detection. Across the entire sampling cruise, Phe displayed the highest average contribution of 52% to $\sum_9$PAH, followed by Flu, which contributed another 44%. Hence, the cumulative contributions of other congeners were less than 5 %. Our results mirror previous results, in that Phe was also the dominant compound among the gas phase PAHs, contributing 50% to Σ_{15}PAH over the North Pacific and Arctic Ocean (Ding et al., 2007).

3.1.2 Decreasing distribution with latitude

Overall, a significant negative correlation was observed between gaseous $\sum_9$PAH and latitude (the coefficients of determination, R^2 was 0.61, the P-value < 0.0010). The partial pressure of seven PAH congeners were calculated by a modified Clausius-Clapeyron equation (Venier et al., 2012), these results were obviously consistent with the trends in concentration with temperature. The mobility of PAHs was usually reduced by decreasing temperature, which contributed to decreasing volatility of PAHs, especially for higher molecular weight PAHs. As shown in Fig. 2, the partial pressure of FluA, Pyr and Chry decreased faster than for the low molecular weight PAHs such as Flu and Phe (All the R^2 and P-values are given in SI). Higher molecular weight PAH congeners were more sensitive to temperature change, in line with expectations for gaseous PAH concentrations with latitude (Fig. 2).

On the other hand, PAHs are more susceptible to photochemical-degradation in the

233   atmosphere. The concentration ratios of Flu to Phe were positively related to latitude (R^2=0.58,

234   P<0.0010) from the North Pacific to the Arctic (Figure 1); and the ratio FluA/(FluA+Pyr) was

235   greater than 0.5 at all stations (Fig. 4). The total photochemical residence time (τ_{total}) of Flu and

236   FluA were derived as 21 and 20 hours, and 9 and 5 hours for Phe and Pyr, respectively (Keyte

237   et al., 2014); the observed low concentrations of Ant in the atmosphere were likely caused by

238   its 2hours of τ_{total}. Furthermore, the atmospheric half-life of Flu is higher than Phe, which

239   means higher removal rates occurred in Phe, and Flu presents a greater transmission potential

240   than Phe for long-range atmospheric transport (LRAT) (Halsall et al., 2001).

241   **3.1.3 Influence of air mass**

242   Diagnostic ratios of gaseous PAHs were calculated, but need to be interpreted with caution,

243   because the ratios might be affected by potential post emission processes. 1-MePhe/Phe in the

244   atmosphere were less than 0.50, implying that the source of the PAHs could be attributed to

245   combustion processes (Yunker et al., 2002; Deka et al, 2016; Wu et al., 2019). This was further

246   supported by the isomeric ratios of FluA/(FluA+Pyr) that ranged from 0.42-0.82; a ratio greater

247   than 0.5 indicates the main sources of grass, wood or coal combustions, and between 0.4 to 0.5

248   usually suggests petrogenic combustion (Qu et al., 2019; Qi et al., 2020).

249   At the mid-latitude sites, the air mass mainly originated from the coast of China, Korea,

250   Japan and Russia, and close-by terrestrial regions as indicated by the air mass back trajectories

251   (Fig. S7 and S8 in SI). With the trajectories of air mass that was used to study the origin of

252   atmospheric PAHs in Japan and other neighboring areas, high concentrations of PAHs and

253   emissions have been already observed in East Asian areas (Ohura et al., 2004; Primbs et al.,

254   2007). Continuously decreasing concentrations of PAHs occurred from the Bering Sea to the

255   Arctic, but increased again between PS-09 and PS-11, where back trajectories indicated the air

256   had passed through Alaska and Siberia, especially on Kamchatka peninsula, consistent with the

257   impact of terrestrial source (Fig. S8 in SI). According to the air mass back trajectories, the

258   source of the atmosphere PAHs in July was significantly affected by the southwest monsoon,

259   which is also an important pathway for long-range transport.

3.2 PAHs in the seawater

3.2.1 PAH profiles in seawater

The concentrations of total freely dissolved $\sum_{11}$PAH in the surface seawater ranged from 1.8 to 16 ng L^{-1} with the mean value of 7.7 $\pm$ 4.6 ng L^{-1}. The maximum concentrations occurred at PS-03 on the northeast coast of Japan, followed by station PS-02 and PS-04, and the minimum was observed at PS-10 in the Bering Strait (Fig. 3, Table S4). A total of 11 different PAHs were regularly detected in the freely-dissolved phase in the seawater samples, including Biph, Flu, Phe, 1-MePhe, Ant, FluA, Pyr, and Chry, BaA, BbF/BkF. The concentrations of higher molecular weight PAHs in seawater were typically below the limits of detection, similar to the atmosphere.

The ratios of 1-MePhe/Phe and FluA/(FluA+Pyr) indicated the main sources of combustions included many types (Yunker et al., 2002; Qu et al., 2019; Qi et al., 2020). The results in seawater were consistent to previous studies in the North Pacific and Arctic Ocean (Ding et al., 2007; Ma et al., 2013).

While Phe also dominated the dissolved $\sum_{11}$PAH, its average contribution was only 36%. Hence more PAHs were regularly present beyond Phe, including Flu, which contributed 25%, FluA (11%), Pyr (10%), in addition 1-MePhe and Biph were 8 % and 5 %, respectively. Other congeners like Ant, BaA, BbF/BkF were only detected in a few of the samples beyond the Bering Sea (for details see SI), whose contributions were less than 4 %. The combined influences of sources like rivers, runoff, currents as well as biogeochemical process cause more higher molecular weight PAHs to be present in the surface seawater (Sambrotto, 1984; McDonough et al., 2014). We speculate that differences in biodegradation and photochemical-degradation of PAHs increased the proportion of higher molecular weight PAHs in seawater (González-Gaya et al., 2019). Bacterial degradation rate constants (K_D) showed a significant inverse correlation with K_{ow}, which means the capacity to biodegrade higher molecular weight and hydrophobic PAHs (i.e., FluA, Pyr, Chry, BbF/BkF) were slower than for lighter weight PAHs (Table S5) (Tucca et al., 2020). Besides, higher molecular weight PAHs in the air sorb to aerosol according their higher octanol-air ratios, contributing to wet and dry deposition entering seawater.

3.2.2 Changes of freely-dissolved PAH distribution with region

Freely dissolved $\sum_{11}$PAH concentrations varied with sampling locations as well, but displayed obvious regional trends instead of correlation with latitude. They ranged from 12 to 16 ng L^{-1} in the Japan Sea to the North Pacific Ocean, located in a mid-latitude temperate zone. Concentration were lower in the nearby Bering Strait ranging only from 1.8 to 4.8 ng L^{-1}, as well as sites in the Arctic Ocean (2.7-6.5 ng L^{-1}). In general, dissolved $\sum_{11}$PAH concentrations closer to shore were relatively higher than those in the open ocean (Fig. 3).

Lower concentrations of seawater Σ_{11}PAH were present at station PS-08, PS-09 and PS-10 in the Bering Strait, which was known as one of the most productive waters in the Arctic Ocean. Likely removal of PAHs by high amounts of biogenic particles significantly decreased the concentration of PAHs in the ocean, where the plankton biomass was higher, consistent with the relevance of the biological pump (González-Gaya et al., 2019). Another reason for low concentrations of Σ_{11}PAH in the Arctic Ocean are the oceans' long residence time, as well as the weak sea ice melting in summer. The ocean current exchange is relatively slow, causing the residence time of surface water to be about 10 years. Melting sea ice has been recognized as an important factor controlling the distribution of PAHs in the Arctic, where only part of the sea ice melts even in summer (MacDonald et al., 2000). The lower salinity supported that continental runoff or melting ice rather than ocean currents were the pathways of PAHs into the surface water, and the atmospheric deposition was also a key source (see below).

3.3 Air-sea exchange of PAHs with two-film model

3.3.1 General net volatilization

The air-sea exchange fluxes of the seven PAHs was generally dominated by net volatilization especially from the North Pacific to the Arctic (Fig. 5, Table S12). Generally, fluxes of the more volatile PAHs especially for Flu and Phe were greater and nearly accounted for >70% of all (Table S12 in SI), based on their dominant contribution to gaseous and free-dissolved PAHs. The maximum values of volatilization and deposition fluxes of Σ_9PAHs were observed at site PS-04 (11 μg m^{-2} day^{-1}) and PS-01 (-2.5 μg m^{-2} day^{-1}) respectively. Flux distributions indicated that the deposition was only observed near land from Shanghai to the Bohai Sea, while net volatilizations were more widespread. For instance, Flu dominated the

318   flux at site PS-04 with the value of 4.2 μg m^{-2} day^{-1}, and Phe at site PS-01 was -5.2 μg m^{-2} day^{-1}

319   ^{1}, due to the greatest concentrations of dissolved Flu at PS-04 and gaseous Phe at PS-01

320   respectively. The effect of volatilization from coastal waters with high PAH levels has reported

321   in other PAH-impacted regions such as the Atlantic, Narragansett Bay (USA) and the southeast

322   Mediterranean (Nizzetto et al., 2008; Castro-Jiménez et al., 2012; Lohmann et al., 2011). The

323   fluxes were mainly contributed by three-ring PAHs, while the fluxes of four-ring PAHs showed

324   less variation in the North Pacific and the Arctic.

325   **3.3.2 Flux trend closely coupling with dissolved phase**

326   The derived air-water exchange fluxes correlated significantly to regional and monthly

327   changes, similar to the freely-dissolved PAH distributions, which might imply the one of driver

328   by concentration gradients between seawater and air (Fig. 5). Volatilizations dominated in the

329   air-sea exchange because the seawater concentrations corrected by K_{aw} were one to three orders

330   of magnitudes higher than equivalent concentrations in the atmosphere.

331   As for individual congeners, there were no clear trends for three-ring PAHs, but diverse

332   ones for higher-ring PAHs, especially FluA and Pyr declined with increasing latitude (Fig. S5

333   in SI). These results verified that higher molecular weight PAHs were more sensitive to changes

334   with temperature. PAHs are moderately volatile and hydrophobic, which facilitates their

335   partitioning from air and water into organic phases (Nizzetto et al., 2010). Obvious outputs of

336   biogenic particles occurred in the Bering Strait and caused a significant decrease in seawater

337   concentration as well as fluxes. In the Arctic, low PAHs fluxes were driven basically by low

338   atmospheric and seawater concentrations. However, the net volatilizations only had a minor

339   impact on atmospheric concentration. According to the long-range transport and diffusion

340   advection of PAHs, the atmospheric concentrations tend to decrease as the latitude increases,

341   so the transports depend largely on temperature changes. In our study, strong correlations were

342   observed for air-sea exchange fluxes with concentrations rather than temperature.

343   **3.4 Implication for the source-sink pattern of PAHs**

344   **3.4.1 Source pattern of PAHs from the Pacific to the Arctic**

345   For further analysis, principal component analysis (PCA) was used to elucidate linear

346   combinations of PAHs, to distinguish between the samples to assess different sources (Nemr et

al., 2005). Two compounds were obtained from PCA, namely the first principal component (PC1) and second principal component (PC2), contributed 74% to the total variance (Fig. 4). Correlation analysis showed high relevance of PC1 for four-ring PAHs, such as FluA and Pyr (r=0.98), FluA and Chry (r=0.90), Pyr and Chry (r=0.94); and PC2 represented mainly three-ring PAHs such as Flu and Phe (r=0.82), Flu and Ant (r=0.56), Phe and 1-MPhe (r=0.67). The scores on PCA showed that all the sites in the Bering Sea and Arctic were concentrated together in the negative axis of PC1 and PC2, while sites in the North Pacific were more dispersed.

The diagnostic ratios and PCA analysis provided qualitative information about the spatial patterns of PAH sources. Based on the analysis mentioned earlier, we inferred that sources of seawater and atmospheric PAHs in the Bering Sea and Arctic were mainly from combustion processes. In the Arctic, the diagnostic ratios of PAH concentrations in seawater were similar to that in atmosphere, which might provide the evidence that PAHs reached high latitudes by long-range atmosphere transport (LRAT). Hence the atmospheric concentrations contributed only low levels in the high latitudes, and combined with sea ice melting, runoff and other biogeochemical process to affect the ratio characteristics. On the other hand, both of the seawater and atmospheric PAHs in the Pacific Ocean were also mainly derived from combustion processes. The difference is that the North Pacific is known as an important cruise routes area, which potentially contributes additional sources factors, complicating the seawater PAHs. Therefore, petroleum combustion emitted by ships is an inevitable source for PAHs in addition to runoff, ocean currents and atmospheric deposition.

3.4.2 Net volatilization prospect under climate changing

Our results illustrated that the majority of PAHs displayed a net volatilization trend from East Asia to the Arctic, which was on the contrary of the previous studies (Zhong et al., 2012; Ma et al., 2013). The significant differences in the fluxes were partly attributed to the different concentrations of gaseous and dissolved PAHs between these two studies whose samples were from different years. The time lag to previous studies might have been sufficient to cause an increase in PAH concentration in surface seawater for the ongoing-emitted PAHs year by year. In addition, East Asia is a possible continental source area and has been estimated to contribute greatly to the global emission inventory of PAHs (Shen et al., 2013). Furthermore, sea surface temperatures (SSTs) in August 2014 were as much as 4 $^{\circ}$C   warmer than the 1982-2010 August

377 mean in the Bering Strait and the sixth smallest Arctic sea ice extent by the satellite record

378 (1979-2014) occurred in the summer of 2014 (Chen et al., 2016), which might partially explain

379 the different results reported here. Lastly, sampling of PAHs by passive sampling only captures

380 freely dissolved or gas-phase compounds, which should lead to air-water exchange fluxes not

381 impacted by inadvertent capture of PAH bound to colloids or small particles.

382   Some persistent organic pollutants, whose primary emissions have been reduced, are

383 suggested having iterative processes (including deposition, volatilization and re-deposition) in

384 the changing Arctic (Cai et al., 2012). Since the ice will prevent the escape of PAHs in winter,

385 we can assume that atmospheric PAHs will deposit in snow and ice by dry/wet deposition

386 processes and the Arctic turned into a sink again. In other words, as a result of global warming

387 with sea ice retreat, whether the polar region is a sink or secondary source depends on the

388 seasonal variety. The air-sea exchange fluxes in our study displayed significantly lower in

389 September than in July (Fig. 5), which might be driven by decreasing temperature and

390 weakened monsoon. PAH concentrations and fluxes are thus likely affected by temporal

391 changes, but more evidence is needed (Fig. S6 in SI). Combining this with our result that fluxes

392 were consistent with surface seawater PAHs concentrations, then seawater might dominate the

393 air-sea exchange when not covered by sea ice. But whether the hypothesis is reasonable or not

394 need to be further studied, and which might determine the role of the Arctic as "sink" or "source"

395 of PAHs.

396 **4 Conclusions**

397   This study focused on the air-sea exchange process of PAHs, relying on LDPEs passive

398 sampling from the North Pacific to Arctic. The gaseous concentrations of $\sum_9$PAH ranged from

399 0.67 to 13 ng m^{-3} and displayed a significant decreasing trend with latitude, which was

400 dominated by long-range transport and photochemical-degradation of PAHs. Different

401 distributions were explained by the air mass back trajectories, coupled with the influence of air-

402 sea exchange and dry/wet deposition processes. The concentrations of total freely dissolved

403 $\sum_{11}$PAH ranged from 1.8 to 16 ng L^{-1} whereas higher molecular weight PAHs showed more

404 presence. The changes in PAH profiles can likely be attributed to their relative capacity to

405 undergo biodegradation and dry/wet deposition. In addition, regional distributions were shown

406   in freely dissolved PAHs, showing high levels in the North Pacific. The lower levels were

407   impacted by biogenic particle removals in the Bering Sea, and were attributed to slow renewal

408   of seawater and melting ice in the Arctic. Molecular ratios of the PAHs in atmosphere and

409   surface seawater indicated combustion sources, and the source indication might provide some

410   evidence for LRAT of high-latitude marine environmental PAHs. Overall, the air-sea fluxes of

411   PAHs presented mostly net volatilizations with special regional and monthly changes,

412   controlled by seawater concentrations. The air-sea exchange process showed only a relatively

413   minor importance of air concentrations, instead the fluxes and dry/wet depositions from

414   atmosphere to seawater might were more important especially in the Arctic.

Reference

Antweiler, R. C., Taylor, H. E., 2008. Evaluation of statistical treatments of left-censored environmental data using coincident uncensored data sets: I. Summary statistics. Environmental Science & Technology, 42(10): 3 732-3 738.

Booij, K., Smedes, F., 2010. An improved method for estimating in situ sampling rates of nonpolar passive samplers. Environmental Science & Technology, 44(17): 6 789-6 794.

Booij, K., Smedes, F., van Weerlee, E. M., 2002. Spiking of performance reference compounds in low density polyethylene and silicone passive water samplers. Chemosphere, 46(8): 1 157-1 161.

Bozlaker, A., Muezzinoglu, A., Odabasi, M., 2008. Atmospheric concentrations, dry deposition and air-soil exchange of polycyclic aromatic hydrocarbons (PAHs) in an industrial region in Turkey. Journal of Hazardous Materials, 153(3): 1 093-1 102.

Cai, M. G., Liu, M. Y., Hong, Q. Q., Lin, J., Huang, P., Hong, J. J., Wang, J., Zhao, W. L., Chen, M., Cai, M. H., Ye, J., 2016. Fate of polycyclic aromatic hydrocarbons in seawater from the Western Pacific to the Southern Ocean (17.5 degrees ^{o}N to 69.2 degrees ^{o}S) and their inventories on the Antarctic Shelf. Environmental Science & Technology, 50(17): 9 161-9 168.

Cai, M. H., Ma, Y. X., Xie, Z. Y., Zhong, G. C., Moeller, A., Yang, H. Z., Sturm, R., He, J. F., Ebinghaus, R., Meng X. Z.,. 2012. Distribution and air-sea exchange of organochlorine pesticides in the North Pacific and the Arctic. Journal of Geophysical Research-Atmospheres, 117: D06311.

Castro-Jiménez, J., Eisenreich, S. J., Mariani, G., Skejo, H., Umlauf G., 2012. Monitoring atmospheric levels and deposition of dioxin-like pollutants in sub-alpine Northern Italy. Atmospheric Environment, 56: 194-202.

Chen, H. W., Alley, R. B., Zhang, F., 2016. Interannual Arctic sea ice variability and associated winter weather patterns: A regional perspective for 1979-2014. Journal of Geophysical Research-Atmospheres, 121(24): 14 433-14 455.

Deka, J., Sarma, K. P., Hoque, R. R., 2016. Source contributions of Polycyclic Aromatic Hydrocarbons in soils around oilfield in the Brahmaputra Valley. Ecotoxicology and Environmental Safety, 133: 281-289.

Ding, X., Wang, X. M., Zhou, Q. X., Cai, H. X., Bi, X. M., Li, G. S., Zheng, M., Guo, Y. S., Jia, M. F., Poeschl, U., 2007. Atmospheric polycyclic aromatic hydrocarbons observed over the North Pacific Ocean and the Arctic area: Spatial distribution and source identification. Atmospheric Environment, 41(10): 2 061-2 072.

Dotel, J., Gong, P., Wang, X. P., Pokhrel, B., Wang, C. F., Nawab, J., 2020. Determination of dry deposition velocity of polycyclic aromatic hydrocarbons under the sub-tropical climate and its implication for regional cycling. Environmental Pollution, 261: 114143.

Draxier, R. R., Hess, G. D., 1998. An overview of the HYSPLIT_4 modelling system for trajectories, dispersion and deposition. Australian Meteorological Magazine, 47(4): 295-308.

Foster, K. L., Stern, G. A., Carrie, J., Bailey, J. N. L., Outridge, P. M., Sanei, H., Macdonald, R. W., 2015.

457   Spatial, temporal, and source variations of hydrocarbons in marine sediments from Baffin Bay,

458   Eastern Canadian Arctic. Science of The Total Environment, 506: 430-443.

459   Friedman, C. L., Selin, N. E., 2012. Long-range atmospheric transport of polycyclic aromatic

460   hydrocarbons: a global 3-D model analysis including evaluation of Arctic sources.

461   Environmental Science & Technology, 46(17): 9 501-9 510.

462   Friedman, C. L., Zhang, Y. X., Selin, N. E., 2014. Climate Change and Emissions Impacts on

463   Atmospheric PAH Transport to the Arctic. Environmental Science & Technology, 48(1): 429-

464   437.

465   Galban-Malagon, C. J., Del Vento, S., Berrojalbiz, N., Ojeda, M. J., Dachs, J., 2013. Polychlorinated

466   biphenyls, hexachlorocyclohexanes and hexachlorobenzene in seawater and phytoplankton

467   from the Southern Ocean (Weddell, South Scotia, and Bellingshausen Seas). Environmental

468   Science & Technology, 47(11): 5 578-5 587.

469   González-Gaya, B., Martinez-Varela, A., Vila-Costa, M., Casal, P., Cerro-Galvez, E., Berrojalbiz, N.,

470   Lundin, D., Vidal, M., Mompean, C., Bode, A., Jimenez, B., Dachs, J., 2019. Biodegradation as

471   an important sink of aromatic hydrocarbons in the oceans. Nature Geoscience, 12: 119-125.

472   Halsall, C. J., Sweetman, A. J., Barrie, L. A., Jones, K. C., 2001. Modelling the behaviour of PAHs during

473   atmospheric transport from the UK to the Arctic. Atmospheric Environment, 35(2): 255-267.

474   Harner, T., Farrar, N., Shoeib, M., Jones, K., Gobas, F., 2003. Characterization of polymer-coated glass

475   as a passive air sampler for persistent organic pollutants. Environmental Science & Technology,

476   37(11): 2 486-2 493.

477   Harvey, H. R., Taylor, K. A., Pie, H. V., Mitchelmore, C. L., 2014. Polycyclic aromatic and aliphatic

478   hydrocarbons in Chukchi Sea biota and sediments and their toxicological response in the Arctic

479   cod, Boreogadus saida. Deep Sea Research Part II: Topical Studies in Oceanography, 102: 32-

480   55.

481   Hung, H., Kallenborn, R., Breivik, K., Su, Y. S., Brorström-Lundén, E., Olafsdottir, K., Thorlacius, J. M.,

482   Leppänen, S., Bossi, R., Skov, H., Mano, S., Patton, G. W., Stern, G., Sverko, E., Fellin, P., 2010.

483   Atmospheric monitoring of organic pollutants in the Arctic under the Arctic Monitoring and

484   Assessment Programme (AMAP): 1993–2006. Science of the Total Environment, 408(15): 2

485   854-2 873.

486   Jaward, F., Farrar, N., Harner, T., Sweetman, A., Jones, K., 2004. Passive air sampling of PCBs, PBDEs,

487   and organochlorine pesticides across Europe. Environmental Science & Technology, 38(1): 34-

488   41.

489   Ke, H. W., Chen, M., Liu, M. Y., Chen, M., Duan, M. S., Huang, P., Hong, J. J., Lin, Y., Cheng, S. Y.,

490   Wang, X. R., Huang, M. X., Cai, M. G., 2017. Fate of polycyclic aromatic hydrocarbons from

491   the North Pacific to the Arctic: Field measurements and fugacity model simulation.

492   Chemosphere, 184: 916-923.

493   Keyte, I. J., Harrison, R. M., Lammel, G., 2014. Chemical reactivity and long-range transport potential

494   of polycyclic aromatic hydrocarbons: A review. Chemical Society Reviews, 45(24): 9 333-9 391.

495   Khairy, M. A., Lohmann, R., 2012. Field validation of polyethylene passive air samplers for parent and

496   alkylated PAHs in Alexandria, Egypt. Environmental Science & Technology, 46(7): 3 990-3 998.

497 Khairy, M. A., Lohmann, R., 2014. Field calibration of low density polyethylene passive samplers for
498   gaseous POPs. Environmental Science -Processes & Impacts, 16(3): 414-421.

499 Laender, F. D., Hammer, J., Hendriks, A. J., Soetaert, K., Janssen, C. R., 2011. Combining monitoring
500   data and modeling identifies PAHs as emerging contaminants in the Arctic. Environmental
501   Science & Technology, 45(20): 9 024-9 029.

502 Lei, P., Zhu, J. J., Pan, K., Zhang, H., 2020. Sorption kinetics of parent and substituted PAHs for low-
503   density polyethylene (LDPE): Determining their partition coefficients between LDPE and water
504   (K-LDPE) for passive sampling. Journal of Environmental Sciences, 87: 349-360.

505 Liss, P. S., Slater, P. G., 1974. Flux of gases across the air-sea interface. Nature, 247: 181-84. Doi:
506   10.1038/247181a0

507 Liu, Y., Wang, S. Y., McDonough, C. A., Khairy, M., Muir, D. C. G., Helm, P. A., Lohmann., R., 2016.
508   Gaseous and freely-dissolved PCBs in the lower Great Lakes based on passive sampling: Spatial
509   trends and air-water exchange. Environmental Science & Technology, 50(10): 4 932-4 939.

510 Lohmann, R., Corrigan, B. P., Howsam, M., Jones, K. C., Ockenden, W. A., 2001. Further developments
511   in the use of semipermeable membrane devices (SPMDs) as passive air samplers for persistent
512   organic pollutants: Field application in a spatial survey of PCDD/Fs and PAHs. Environmental
513   Science & Technology, 35(12): 2 576-2 582.

514 Lohmann, R., Dapsis, M., Morgan, E. J., Dekany, V., Luey, P. J., 2011. Determining air-water exchange,
515   spatial and temporal trends of freely dissolved PAHs in an urban estuary using passive
516   polyethylene samplers. Environmental Science & Technology, 45(7): 2 655-2 662.

517 Ma, J. M., Hung, H., Tian, C. G., Kallenborn, R., 2011. Revolatilization of persistent organic pollutants
518   in the Arctic induced by climate change. Nature Climate Change, 1(5): 255-260.

519 Ma, Y. X., Xie, Z. Y., Yang, H. Z., Möller, A., Halsall, C., Cai, M. H., Sturm, R., Ebinghaus, R., 2013.
520   Deposition of polycyclic aromatic hydrocarbons in the North Pacific and the Arctic. Journal of
521   Geophysical Research Atmospheres, 118(11): 5 822-5 829.

522 MacDonald, R. W., Barrie, L. A., Bidleman, T. F., Diamond, M. L., Gregor, D. J., Semkin, R. G., Strachan,
523   W. M. J.,. Li, Y. F, Wania, F., Alaee, M., Alexeeva, L. B., Backus, S. M., Bailey, R., Bewers, J.
524   M., Gobeil, C., Halsall, C. J., Harner, T., Hoff, J. T., Jantunen, L. M. M., Lockhart, W. L., Mackay,
525   D., Muir, D. C. G., Pudykiewicz, J., Reimer, K. J., Smith, J. N., Stern, G. A., Schroeder, W. H.,
526   Wagemann, R., Yunker, M. B., 2000. Contaminants in the Canadian Arctic: 5 years of progress
527   in understanding sources, occurrence and pathways. Science of the Total Environment, 254(2-
528   3): 93-234.

529 Mayer, P., Toll, J., Hermens, L., Mackay, D., 2003. Equilibrium sampling devices. Environmental
530   Science & Technology, 37(9): 184A-191A.

531 McDonough, C. A., Khairy, M. A., Muir, D. C. G., Lohmann, R., 2014. Significance of population centers
532   as sources of gaseous and dissolved PAHs in the Lower Great Lakes. Environmental Science &
533   Technology, 48(14): 7 789-7 797.

534 Meijer, S. N., Shoeib, M., Jantunen, L. M. M., Jones, K. C., Harner, T., 2003. Air-soil exchange of

535   organochlorine pesticides in agricultural soils. 1. Field measurements using a novel in situ

536   sampling device. Environmental Science & Technology, 37(7): 1 292- 1 299.

537 Mulder, M. D., Angelika H., Kukučka, P., Kuta, J., Přibylová, P., Prokeš, R., Lammel, G., 2015. Long-

538   range atmospheric transport of PAHs, PCBs and PBDEs to the central and eastern Mediterranean

539   and changes of PCB and PBDE congener patterns in summer 2010. Atmospheric Environment,

540   111: 51-59.

541 Nemr, A. E., Khaled, A., El-Sikaily, A., Said, T. O., Abd-Allah, A. M. A., 2005. Distribution and sources

542   of polycyclic aromatic hydrocarbons in surface sediments of the Suez Gulf. Environmental

543   Monitoring and Assessment, 111: 333-358.

544 Nizzetto, L., Lohmann, R., Gioia, R., Jahnke, A., Temme, C., Dachs, J., Herckes, P., Di Guardo, A., Jones

545   K. C., 2008. PAHs in air and seawater along a North-South Atlantic transect: Trends, processes

546   and possible sources. Environmental Science & Technology, 42(5): 1 580-1 585.

547 Nizzetto, L., Macleod, M., Borga, K., Cabrerizo, A., Dachs, J., Di Guardo, A., Ghirardello, D., Hansen,

548   K. M., Jarvis, A., Lindroth, A., Ludwig, B., Monteith, D., Perlinger, J. A., Scheringer, M.,

549   Schwendenmann, L., Semple, K. T., Wick, L. Y., Zhang, G., Jones, K. C., 2010. Past, present,

550   and future controls on levels of persistent organic pollutants in the global environment.

551   Environmental Science & Technology, 44(17): 6 526-6 531.

552 Ohura, T., Amagai, T., Fusaya, M., Matsushita, H., 2004. Spatial distributions and profiles of atmospheric

553   polycyclic aromatic hydrocarbons in two industrial cities in Japan. Environmental Science &

554   Technology, 38(1): 49-55.

555 Okona-Mensah, K. B., Battershill, J., Boobis, A., Fielder, R., 2005. An approach to investigating the

556   importance of high potency polycyclic aromatic hydrocarbons (PAHs) in the induction of lung

557   cancer by air pollution. Food and Chemical Toxicology, 43: 1 103-1 116.

558 Perera, F., Tang, D. L., Whyatt, R., Lederman, S. A., Jedrychowski, W., 2005. DNA damage from

559   polycyclic aromatic hydrocarbons measured by benzo[a]pyrene-DNA adducts in mothers and

560   newborns from Northern Manhattan, the World Trade Center Area, Poland, and China. Cancer

561   Epidemiology Biomarkers & Prevention, 14(3): 709-714.

562 Primbs, T., Simonich, S., Schmedding, D., Wilson, G., Jaffe, D., Takami, A., Kato, S., Hatakeyama, S.,

563   Kajii, Y., 2007. Atmospheric outflow of anthropogenic semivolatile organic compounds from

564   East Asia in spring 2004. Environmental Science & Technology, 41(10): 3 551-3 558.

565 Qi, P. Z., Qu, C. K., Albanese, S., Lima, A., Cicchella, D., Hope, D., Cerino, P., Pizzolante, A., Zheng,

566   H., Li, J. J., De Vivo, B., 2020. Investigation of polycyclic aromatic hydrocarbons in soils from

567   Caserta provincial territory, southern Italy: Spatial distribution, source apportionment, and risk

568   assessment. Journal of Hazardous Materials, 383: 121158.

569 Qu, C. K., Albanese, S., Lima, A., Hope, D., Pond, P., Fortelli, A., Romano, N., Cerino, P., Pizzoante, A.,

570   De Vivo, B., 2019. The occurrence of OCPs, PCBs, and PAHs in the soil, air, and bulk deposition

571   of the Naples metropolitan area, southern Italy: Implications for sources and environmental

572   processes. Environment International, 124: 89-97.

573 Sambrotto, R. N., Goering, J. J., McRoy, C. P., 1984. Large yearly production of phytoplankton in the

574   Western Bering Strait. Science, 225(4 667): 1 147-1 150.

575   Shaw, M., Mueller, J. F., 2009. Time integrative passive sampling: how well do chemcatchers integrate

576   fluctuating pollutant concentrations? Environmental Science & Technology, 43(5): 1 443-1 448.

577   Shen, H. Z., Huang, Y., Wang, R., Zhu, D., Li, W., Shen, G. F., Wang, B., Zhang, Y. Y., Chen, Y. C., Lu,

578   Y., Chen, H., Li, T. C., Sun, K., Li, B. G., Liu, W. X., Liu, J. F., Tao, S., 2013. Global atmospheric

579   emissions of polycyclic aromatic hydrocarbons from 1960 to 2008 and future predictions.

580   Environmental Science & Technology, 47(12): 6 415-6 424.

581   Stabeno, P. J., Van Meurs, P., 1999. Evidence of episodic on-shelf flow in the southeastern Bering Sea.

582   Journal of Geophysical Research-Oceans, 104(C12): 29 715-29 720.

583   Stuer-Lauridsen, F. 2005. Review of passive accumulation devices for monitoring organic

584   micropollutants in the aquatic environment. Environmental Pollution, 136(3): 503-524.

585   Tucca, F., Luarte, T., Nimptsch, J., Woelfl, S., Pozo, K., Casas, G., Dachs, J., Barra, R., Chiang, G.,

586   Galban-Malagon, C., 2020. Sources and diffusive air-water exchange of polycyclic aromatic

587   hydrocarbons in an oligotrophic North-Patagonian lake. Science of the Total Environment, 738:

588   139838.

589   Venier, M., Hung, H., Tych, W., Hites, R. A., 2012. Temporal trends of persistent organic pollutants: A

590   comparison of different time series models. Environmental Science & Technology, 46(7): 3 928-

591   3 934.

592   Wania, F., Shunthirasingham, C., 2020. Passive air sampling for semi-volatile organic chemicals.

593   Environmental Science-Processes & Impacts, 22(10): 1 925-2 002.

594   Woodgate, R. A., Aagaard, K., Weingartner, T. J., 2005. A year in the physical oceanography of the

595   Chukchi Sea: Moored measurements from autumn 1990-1991. Deep-Sea Research Part II-

596   Topical Studies In Oceanography, 52(24-26): 3 116-3 149.

597   Wu X. W., Wang, Y., Zhang, Q. N., Zhao, H. X., Yang, Y., Zhang, Y. W., Xie, Q., Chen, J. W., 2019.

598   Seasonal variation, air-water exchange, and multivariate source apportionment of polycyclic

599   aromatic hydrocarbons in the coastal area of Dalian, China. Environmental Pollution, 244: 405-

600   413.

601   Yunker, M. B., Macdonald, R. W., Vingarzan, R., Mitchell, R. H., Goyette, D., Sylvestre, S., 2002. PAHs

602   in the Fraser River basin: A critical appraisal of PAH ratios as indicators of PAH source and

603   composition. Organic Geochemistry, 33(4): 489-515.

604   Yunker, M. B., Macdonald, R. W., Snowdon, L. R., Fowler, B. R., 2011. Alkane and PAH biomarkers as

605   tracers of terrigenous organic carbon in Arctic Ocean sediments. Organic Geochemistry, 42(9):

606   1 109-1 146.

607   Zhao, W. L., Cai, M. G., Adelman, D., Khairy, M., August, P., Lohmann, R., 2018. Land-use-based

608   sources and trends of dissolved PBDEs and PAHs in an urbanized watershed using passive

609   polyethylene samplers. Environmental Pollution, 238: 573-580.

610   Zhong, G. C., Xie, Z. Y., Cai, M. H., Moeller, A., Sturm, R., Tang, J. H., Zhang, G., He, J. F., Ebinghaus,

611   R., 2012. Distribution and air-sea exchange of current-use pesticides (CUPs) from East Asia to

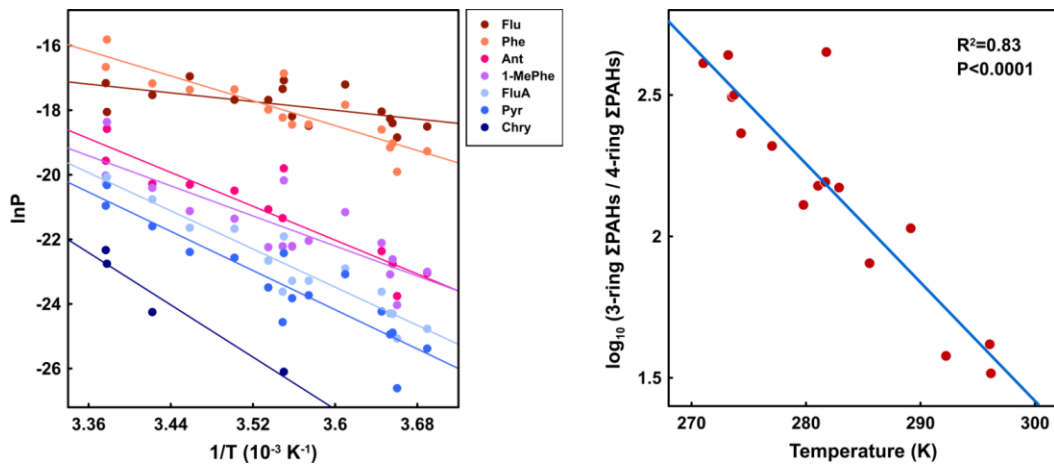612   the high Arctic Ocean. Environmental Science & Technology, 46(1): 259-267.

613
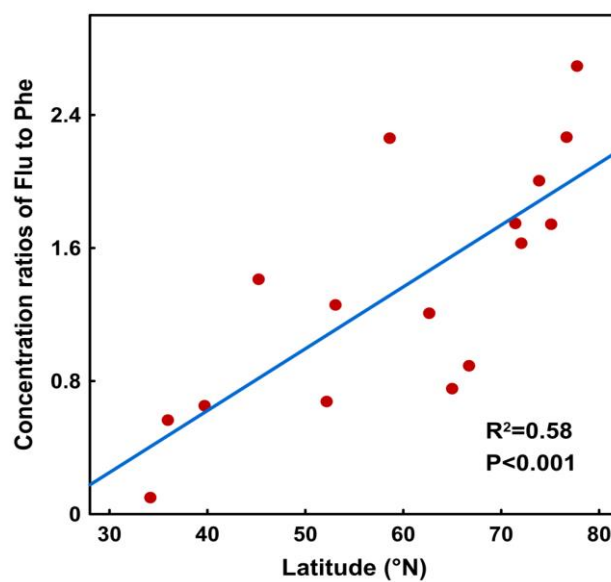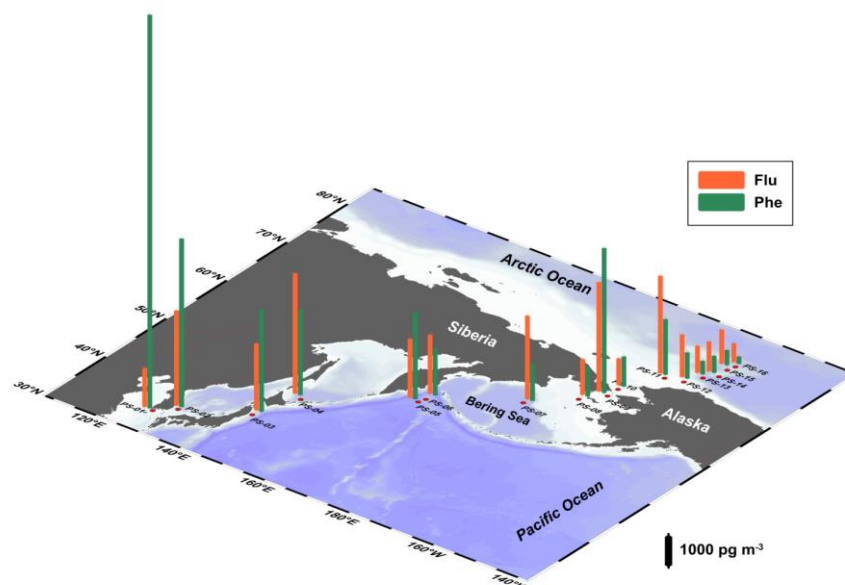
Fig. 1. The gaseous concentration distribution of Flu and Phe along the cruise transect
(the figure above), and the ratios of Flu to Phe as a function to latitude (the figure
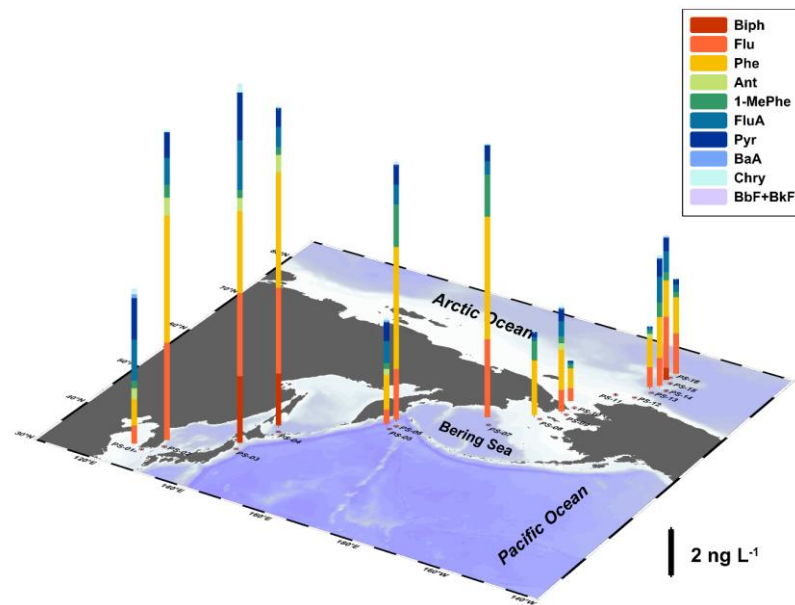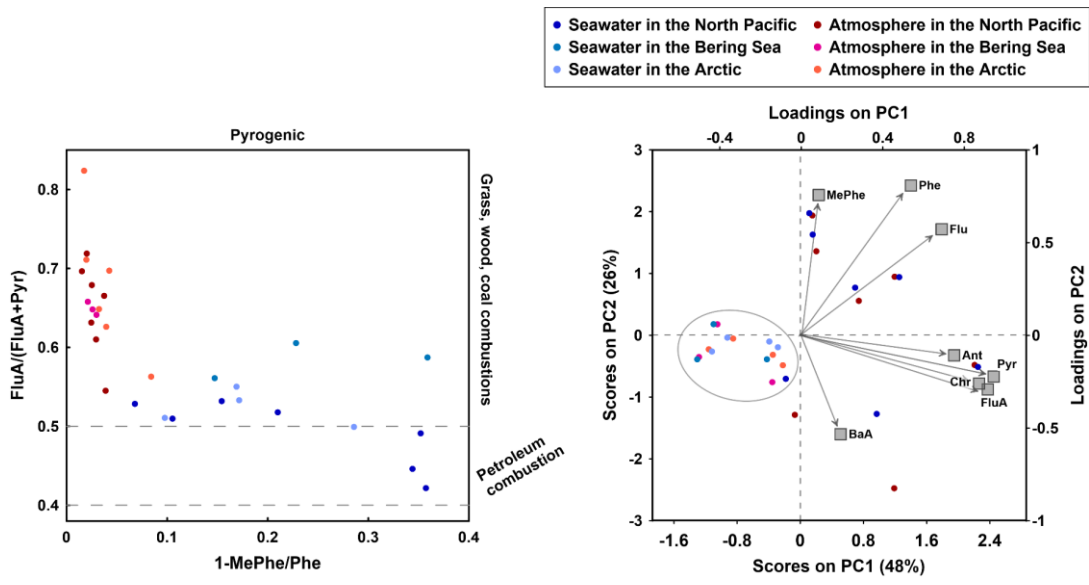below). (The domination of Flu and Phe presented in Fig. S3)

617

618

619　**Fig. 2. The partial pressure of PAH congeners as a function of water temperature (left),**

620　　**and the ratios of the sum of three-ring PAHs to four-ring PAHs as a function of air**

621　　　　　　　　　　　　　　**temperature (right).**

622

623

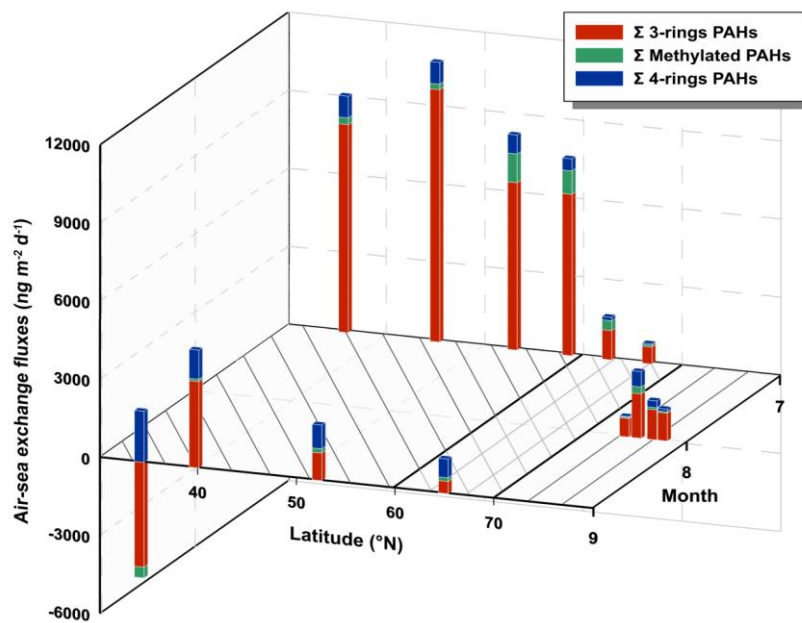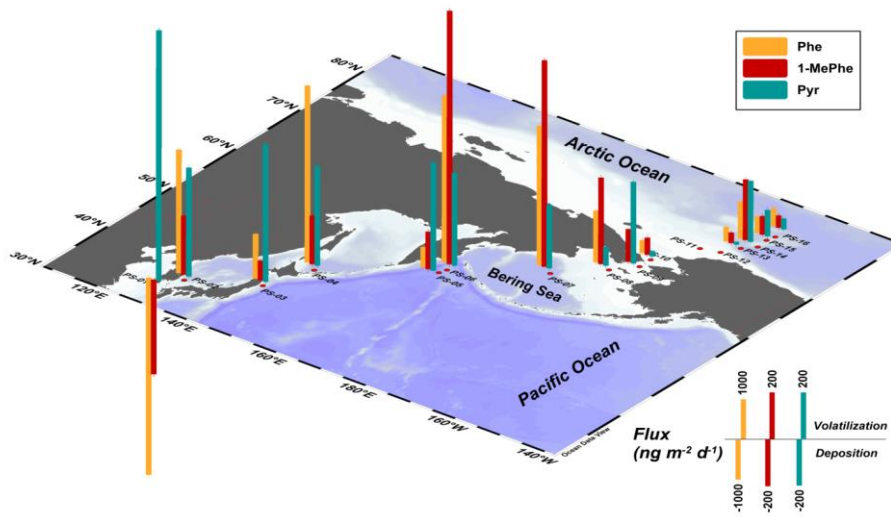624　　　**Fig. 3. The PAH concentrations in surface seawater along the cruise transect.**

625

626

Fig. 4. Results of PAH diagnostic ratios of MePhe/Phe and FluA/(FluA+Pyr) (left),

and PCA (right) for samples in seawater (dots in blue) and atmosphere (dots in red).

629

Fig. 5. The distribution of PAH air-sea exchange fluxes, and their monthly changes.

631